Research Article | Vol. 25, No. 4 | 20 Feb 2017 | OPTICS EXPRESS 3553

Optics EXPRESS

Measurement of third-order nonlinearities in selected solvents as a function of the pulse width

MARIA L. MIGUEZ,[1] TIAGO G. B. DE SOUZA,[1] EMERSON C. BARBANO,[1] SERGIO C. ZILIO,[1,2] AND LINO MISOGUTI[1,*]

[1]*Instituto de Física de São Carlos, Universidade de São Paulo, CP 369, 13560-970 São Carlos, SP, Brazil*

[2]*Universidade Federal de Uberlândia, Av. João Naves de Ávila 2121, 38400-902 Uberlândia, MG, Brazil*

[*]*misoguti@ifsc.usp.br*

Abstract: We investigated the magnitude and origin of the nonlinear refraction in several solvents with the nonlinear ellipse rotation measurements as a function of the pulse duration in the range from 60fs to 2ps. Due to the presence of non-instantaneous nuclear contributions concurrently with the nearly instantaneous electronic nonlinearity, solvents present effective refractive nonlinearities that depend on the pulse duration. By proposing an empirical model where the nonlinearity grows exponentially with the pulse duration normalized to the response time, we could separate contributions from fast isotropic and slow nuclear reorientational nonlinearities. *Z*-scan measurements were also carried out to support our model.

OCIS codes: (190.4400) Nonlinear optics, materials; (190.3270) Kerr effect; (320.7110) Ultrafast nonlinear optics.

References and links

1. D. McMorrow, W. T. Lotshaw, and G. A. Kenney-Wallace, "Femtosecond optical Kerr studies on the origin of the nonlinear responses in simple liquids," IEEE J. Quantum Electron. **24**(2), 443–454 (1988).
2. P. Langot, S. Montant, and E. Freysz, "Measurement of non-instantaneous contribution to the $\chi^{(3)}$ in different liquids using femtosecond chirped pulses," Opt. Commun. **176**(4–6), 459–472 (2000).
3. J. Burgin, C. Guillon, and P. Langot, "Femtosecond investigation of the non-instantaneous third-order nonlinear susceptibility in liquids and glasses," Appl. Phys. Lett. **87**(21), 211916 (2005).
4. K. Polok, W. Gadomski, and B. Ratajska-Gadomska, "Femtosecond optical Kerr effect setup with signal "live view" for measurements in the solid, liquid, and gas phases," Rev. Sci. Instrum. **86**(10), 103109 (2015).
5. M. Reichert, H. Hu, M. R. Ferdinandus, M. Seidel, P. Zhao, T. R. Ensley, D. Peceli, J. M. Reed, D. A. Fishman, S. Webster, D. J. Hagan, and E. W. Van Stryland, "Temporal, spectral, and polarization dependence of the nonlinear optical response of carbon disulfide," Optica **1**(6), 436–445 (2014).
6. M. Reichert, H. Hu, M. R. Ferdinandus, M. Seidel, P. Zhao, T. R. Ensley, D. Peceli, J. M. Reed, D. A. Fishman, S. Webster, D. J. Hagan, and E. W. Van Stryland, "Temporal, spectral, and polarization dependence of the nonlinear optical response of carbon disulfide: erratum," Optica **3**(6), 657–658 (2016).
7. T. H. Huang, C. C. Hsu, T. H. Wei, S. Chang, S. M. Yen, C. P. Tsai, R. T. Liu, C. T. Kuo, W. S. Tse, and C. Chia, "The transient optical Kerr effect of simple liquids studied with an ultrashort laser with variable pulsewidth," IEEE J. Sel. Top. Quantum Electron. **2**(3), 756–768 (1996).
8. B. Gu, H. T. Wang, and W. Ji, "*Z*-scan technique for investigation of the noninstantaneous optical Kerr nonlinearity," Opt. Lett. **34**(18), 2769–2771 (2009).
9. R. A. Ganeev, A. I. Ryasnyansky, M. Baba, M. Suzuki, N. Ishizawa, M. Turu, S. Sakakibara, and H. Kuroda, "Nonlinear refraction in CS_2," Appl. Phys. B **78**(3–4), 433–438 (2004).
10. X. Q. Yan, X. L. Zhang, S. Shi, Z. B. Liu, and J. G. Tian, "Third-order nonlinear susceptibility tensor elements of CS_2 at femtosecond time scale," Opt. Express **19**(6), 5559–5564 (2011).
11. I. Rau, F. Kajzar, J. Luc, B. Sahraoui, and G. Boudebs, "Comparison of *Z*-scan and THG derived nonlinear index of refraction in selected organic solvents," J. Opt. Soc. Am. B **25**(10), 1738–1747 (2008).
12. M. R. Ferdinandus, M. Reichert, T. R. Ensley, H. Hu, D. A. Fishman, S. Webster, D. J. Hagan, and E. W. Van Stryland, "Dual-arm *Z*-scan technique to extract dilute solute nonlinearities from solution measurements," Opt. Mater. Express **2**(12), 1776–1790 (2012).
13. M. L. Miguez, E. C. Barbano, S. C. Zilio, and L. Misoguti, "Accurate measurement of nonlinear ellipse rotation using a phase-sensitive method," Opt. Express **22**(21), 25530–25538 (2014).

#283446 https://doi.org/10.1364/OE.25.003553
Journal © 2017 Received 22 Dec 2016; revised 3 Feb 2017; accepted 3 Feb 2017; published 9 Feb 2017

Optics EXPRESS

14. M. L. Miguez, E. C. Barbano, J. A. Coura, S. C. Zilio, and L. Misoguti, "Nonlinear ellipse rotation measurements in optical thick samples," Appl. Phys. B **120**(4), 653–658 (2015).
15. R. W. Boyd, *Nonlinear Optics*, 3rd ed. (Academic, 2008).
16. D. Milam, "Review and assessment of measured values of the nonlinear refractive-index coefficient of fused silica," Appl. Opt. **37**(3), 546–550 (1998).
17. M. Sheik-Bahae, A. A. Said, T. Wei, D. J. Hagan, and E. W. Van Stryland, "Sensitive measurement of optical nonlinearities using a single beam," IEEE J. Quantum Electron. **26**(4), 760–769 (1990).
18. X. Q. Yan, Z. B. Liu, X. L. Zhang, W. Y. Zhou, and J. G. Tian, "Polarization dependence of *Z*-scan measurement: theory and experiment," Opt. Express **17**(8), 6397–6406 (2009).
19. E. C. Barbano, T. G. B. de Souza, S. C. Zilio, and L. Misoguti, "Comparative study of electronic and orientational nonlinear refractive indices with nonlinear ellipse rotation measurements," J. Opt. Soc. Am. B **33**(12), E40–E44 (2016).
20. A. Owyoung, "Ellipse rotation studies in laser host materials," IEEE J. Quantum Electron. **9**(11), 1064–1069 (1973).
21. M. Lefkir and G. Rivoire, "Influence of transverse effects on measurement of third-order nonlinear susceptibility by self-induced polarization state changes," J. Opt. Soc. Am. B **14**(11), 2856–2864 (1997).
22. P. O'Shea, M. Kimmel, X. Gu, and R. Trebino, "Highly simplified device for ultrashort-pulse measurement," Opt. Lett. **26**(12), 932–934 (2001).
23. K. Iliopoulos, D. Potamianos, E. Kakkava, P. Aloukos, I. Orfanos, and S. Couris, "Ultrafast third order nonlinearities of organic solvents," Opt. Express **23**(19), 24171–24176 (2015).
24. M. B. M. Krishna and D. N. Rao, "Influence of solvent contribution on nonlinearities of near infra-red absorbing croconate and squaraine dyes with ultrafast laser excitation," J. Appl. Phys. **114**(13), 133103 (2013).

1. Introduction

Molecular solvents usually present third-order nonlinear refractive indices with mixed electronic and nuclear contributions that respectively have nearly instantaneous and slow temporal responses [1–8]. In order to study them, time-resolved techniques such as pump-probe [4] are the most appropriate to follow the time evolution of the nonlinear response and to separate each individual contribution. It is known that there are three major nuclear mechanisms, which in decreasing magnitude degree are: diffusive reorientation, libration and intermolecular collision-induced molecular polarizability variation, each one with its own response time [5,6]. Due to the large number of variables and the complexity to obtain them, there is a lack of experimental data for most solvents, except for CS_2, which has been extensively studied for a long time [1,9] and is known to present a strong non-instantaneous third-order nonlinear response resulting in a pulse width dependence [5,6]. Most of the works study n_2 at fixed time regimes, with different laser systems that operate either at femtosecond (fs) [9,10], picosecond (ps) [9,11] or nanosecond (ns) [9] regimes. The effective refractive nonlinearity, $n_{2,eff}$, changes with the pulse duration. Therefore, in order to have the correct interpretation of the nonlinear interaction with a pulsed laser is crucial to know how the material response depends on the pulse width, especially for ultrashort pulses because chirp usually causes drastic changes. In addition, to characterize the nonlinearity of solutions, it is important to know the contribution of the solvent to separate the signal arising just from the solute [12].

Recently, we developed a single beam method to precisely measure optical nonlinearity by means of the nonlinear ellipse rotation (NER) effect [13,14]. For isotropic samples, the NER signal is related to one independent element of the $\chi^{(3)}$ tensor, $B = 6\chi_{1221}$, regardless of the polarization state of the beam [15]. In addition, NER measurements using thick samples also permit discriminate two or more samples in a single scan, improving comparative measurements [14]. A reference sample can be scanned with an unknown sample and their nonlinear magnitudes can immediately be compared. However, single beam techniques such as NER, are not suitable, in principle, to measure response times of dynamic signals, and so, two beams are usually employed. Nevertheless, the single beam configuration is simpler and enables a higher precision for magnitude determination. With this in mind, one could think in changing the pulse duration to extract information about the dynamics. Indeed, this is possible for samples that present slow effects because the effective nonlinearity changes with the pulse width. In particular, we show here that the single beam NER measurement [13,14], can be

Optics EXPRESS

employed as a function of pulse width to study several solvents. A Ti:sapphire laser system is used to generate pulses with durations from ~60 fs to ~2 ps that are incident into a silica cuvette containing the solvent in the thick sample condition. A reference signal is provided by the fused silica of the cuvette walls because it is a well-known calibration material, having only the fast electronic nonlinearity ($n_2 \approx 2.5 \times 10^{-20}$ m^2/W, $B \approx 3.7 \times 10^{-22}$ m^2/V^2) [15,16] which is constant in the range of pulse widths employed. For the solvents measured here, the NER signal (B values) grows as the pulse width increases due to the contribution of the slow nuclear nonlinearity. The pulse width behavior could be adjusted by a simple empirical expression that considers both fast isotropic and slow reorientacional responses. Although very simple, this model allows to find the other tensor element, $A = 6\chi_{1122}$, and consequently, combinations such as $A + B/2$, responsible for the usual n_2 observed when linear polarization is employed. As already mentioned, CS_2 is a well-characterized solution and was used to test our model. Also, Z-scan measurements [17] using linear and circular polarization [18,19] were performed to give support to our results.

2. Nonlinear refraction of solvents

The origin of the nonlinear refractive index in solvents has two main contributions - one practically instantaneous due to bound electrons, and other non-instantaneous that is related to the nuclei, mostly due to molecular reorientation. It is possible to describe the change in the refractive index for a single beam as [5]:

$$\Delta n(t) = n_{2,el} I(t) + \int_{-\infty}^{\infty} R(t-t') I(t') dt', \tag{1}$$

where $n_{2,el}$ is the electronic nonlinearity, $I(t)$ is the irradiance and $R(t)$ is the non-instantaneous component of the third-order response. As mentioned, organic solvents as CS_2 usually present three nuclear contributions known as diffusive reorientation, libration and collision. The first two are polarization dependent, but the collision term is isotropic like the electronic nonlinearity, as discussed in Ref [5]. So, the nuclear contribution is the sum of these three contributions:

$$R(t) = \sum_m n_{2,m} r_m(t), \tag{2}$$

where $n_{2,m}$ is the magnitude of the m^{th} mechanism and $r_m(t)$ is the temporal response function. If a pulsed laser is employed in nonlinear refractive index measurements, the time averaged index change may be written as:

$$\langle \Delta n(t) \rangle = \frac{\int \Delta n(t) I(t) dt}{\int I(t) dt}, \tag{3}$$

where the integral is carried out over the pulse duration. Using Eq. (1) one can write the effective nonlinearity as:

$$n_{2,eff} = n_{2,el} + \frac{\int I(t) \int R(t-t') I(t') dt' dt}{\int I^2(t) dt}. \tag{4}$$

It is possible to calculate the pulse width dependence of $n_{2,eff}$ for both linear and circular polarizations using known parameters of the third-order response of a particular material (r_m, $n_{2,m}$ and respective response times) and Eq. (4). Except for CS_2, the magnitude and response time of nonlinear effects of most solvents are in general seldom found in the literature, making it difficult to calculate $n_{2,eff}$ over a range of pulse widths. To circumvent this lack of data, we propose an empirical model explaining the pulse width dependence in any solvent which has contributions from the fast isotropic ($n_{2,fast}$) and the slow reorientational ($n_{2,slow}$)

Optics EXPRESS

nonlinearities. For simplicity, in this work we consider that *fast* and *slow* nonlinearities are respectively associated to *isotropic* (pure electronic + collision) and the *reorientational* (libration + diffusive) processes. This model assumes that:

$$n_{2,eff} = n_{2,fast} + n_{2,slow}\left(1-\exp\left(\frac{-\tau}{\tau_0}\right)\right), \tag{5}$$

where τ is the pulse width and τ_0 is one characteristic response time of the solvent nonlinearity.

It is interesting to point out the relation between the nonlinear refractive index and the susceptibility components, A and B. For linear polarization, n_2 is given by [19]:

$$n_2 = \frac{3\chi_{1111}}{4n_0^2\varepsilon_0 c} = \frac{3}{4n_0^2\varepsilon_0 c}\left(\frac{A}{3}+\frac{B}{6}\right) = \frac{1}{4n_0^2\varepsilon_0 c}\left(A+\frac{B}{2}\right), \tag{6}$$

where, ε_0 is the vacuum permittivity, c is the speed of light and n_0 is the linear refractive index. Depending if the nonlinearity has an isotropic or reorientational origin, $A = B$ or $B = 6A$, respectively [15]. Therefore, using a specific subscript to distinguish the origin of the nonlinearity, we have $A_{fast} = B_{fast}$, and $B_{slow} = 6A_{slow,}$ and consequently for nonlinear refractive index [19]:

$$n_{2,fast} = \frac{3}{8}\frac{B_{fast}}{n_0^2\varepsilon_0 c} = \frac{3}{8}\frac{A_{fast}}{n_0^2\varepsilon_0 c}, \tag{7}$$

for an isotropic symmetry nonlinearity and:

$$n_{2,slow} = \frac{1}{6}\frac{B_{slow}}{n_0^2\varepsilon_0 c} = \frac{A_{slow}}{n_0^2\varepsilon_0 c}, \tag{8}$$

for a reorientational nonlinearity.

Similar to Eq. (5), it is possible to express other effective nonlinear susceptibilities, B_{eff} and A_{eff}, with the appropriate *fast* and *slow* terms and their correct conversion relations. For instance, in NER measurements we measure only B_{eff} and using the Eq. (5) and Eqs. (7) and (8), we have:

$$B_{eff} = B_{fast} + B_{slow}\left(1-\exp\left(\frac{-\tau}{\tau_0}\right)\right). \tag{9}$$

For the other nonlinear susceptibility, A_{eff}, we have,

$$A_{eff} = A_{fast} + A_{slow}\left(1-\exp\left(\frac{-\tau}{\tau_0}\right)\right) = B_{fast} + \frac{B_{slow}}{6}\left(1-\exp\left(\frac{-\tau}{\tau_0}\right)\right). \tag{10}$$

As shown, it is possible to obtain any curve with this model, including the nonlinear susceptibility related to $n_{2,eff}$ for linear polarization, $A_{eff} + B_{eff}/2$, Eq. (6), as well as the curve for A_{eff} which can be obtained from $n_{2,eff}$ measurements using a circularly polarized beam [15]. *Z*-scan measurements can be used for $n_{2,eff}$ determination for linear and circular polarizations. With these measurements, we have an interesting ratio dependence Δn(linear)/Δn(circular) which can be used to establish the contributions of isotropic or reorientational nonlinearities, if the ratio is closer to 1.5 or 4 [19], respectively. We can test the empirical model with CS_2 by calculating $n_{2,eff}$ using Eq. (4) and using the parameters found in the Ref [6].

Optics EXPRESS

3. Nonlinear ellipse rotation and *Z*-scan

Z-scan is a well-established technique for measuring refractive n_2. It explores the Kerr-lens effect and can determine both the magnitude and sign of optical nonlinear refraction. Its success is due to the simplicity of the single beam approach, and most of the theory and experimental details are already described in the literature [17].

Another interesting effect related to the third-order nonlinear refraction in isotropic media is the nonlinear rotation of an elliptically polarized laser beam [20]. For an isotropic sample, there are only two independent elements represented by the coefficients A (= $6\chi_{1122}$ or = $3\chi_{1122} + 3\chi_{1212}$) and B (= $6\chi_{1221}$) [15]. Their ratios are intrinsically dependent on the physical origin of the nonlinearity. For instance, $B/A = 6$ for an orientational nonlinearity, while $B/A = 1$ for a pure non-resonant electronic and $B/A = 0$ for electrostriction and thermal nonlinearity. As already mentioned, we developed a technique for measuring NER signals with high precision by means of a phase-sensitive method in thick samples using a short focus lens [14]. In this case, the sample can be probed more locally and also, it is possible to simultaneously measure more than one sample in a single run. For instance, in the case of the cuvette filled with solvent, it is possible to measure the signal of the solvent and concomitantly, the two silica walls which provide reference signals. This single beam measurement allows direct magnitude comparison and better signal-to-noise ratio since both samples are probed under the same laser conditions. Furthermore, due to the open-aperture configuration, this method is less sensitive to the beam transverse mode and the sample surface quality. The theoretical details for the NER measurement using a dual-phase locking for thin and thick sample can be found elsewhere [13,14]. Here we choose to work with thick sample because it provides a type of self-referenced method where in a single measurement we can determine the signal from an unknown and a reference samples. Basically, for thick sample the ellipse rotation angle as a function of sample position is [14]:

$$\left\langle \alpha(z) \right\rangle_{lock-in} = \frac{\omega \sin 2\phi B}{8 n_0^2 \varepsilon_0 c^2} (n_0 z_R) \frac{I_0}{\sqrt{2}} \left[\tan^{-1}(z_b / z_R) - \tan^{-1}(z_a / z_R) \right], \qquad (11)$$

where $z_b = z + L/(2n_0)$ and $z_a = z\text{-}L/(2n_0)$, L is the sample thickness, n_0 is the linear index of refraction, z_R is the Rayleigh length, ϕ is the angle of the quarter-waveplate ($\lambda/4$) used to produce the elliptical polarized beam ($\phi = 22.5°$ for better signal-to-noise ratio [13]) and ω is the frequency of the laser. Since NER measurements are performed with pulsed lasers, it is necessary to consider the time-averaged laser intensity, which for a temporal Gaussian pulse is $I = I_0/\sqrt{2}$ [17] and also, Gaussian beam spatial profile, $I(z = 0) = I/2$ [21], as already considered in Eq. (11). Here, B is B_{eff} since, depending of the pulse width, different nonlinear mechanisms contribute to the NER signal on the lock-in amplifier, $\langle\alpha\rangle_{lock\text{-}in}$.

A commercial Ti:sapphire multipass chirped-pulse-amplifier system (Dragon, K&M Labs) was used to generate 790 nm pulses with tunable duration, by using the internal grating pair of the pulse compressor. The bandwidth limited pulse of this laser is about 35 fs (FWHM). The experimental setup for NER and *Z*-scan are very similar, except for the fact that *Z*-scan uses the thin sample condition and the thick sample condition was employed for NER. In both cases, the sample is translated along the *z*-direction. We also added a $\lambda/4$ plate to control de beam ellipticity. Another difference between the two techniques is that the *Z*-scan works with a small aperture and NER in an open-aperture configuration that allows all light to be collected into the photodetector with a lens placed after the sample.

The cuvette (2 mm path-length) filled with solvent is scanned through the focus of the laser beam at $z = 0$, being z negative (positive) for the sample located at the pre-focal (post-focal) position. The laser is focused into the sample with a $f = 150$ mm, $z_R \approx 1.6$ mm ($f = 30$ mm, $z_R \approx 0.05$ mm) focal length lens for *Z*-scan (NER).

Optics EXPRESS

4. Experimental results

To test the proposed model, we characterized 7 common organic solvents, namely CS_2, toluene, chloroform, acetone, ethanol, methanol, and DMSO (dimethylsulfoxide), also including water. These solvents provide a broad selection of temporal responses and magnitude of the *isotropic* and the *reorientational* nonlinearities. We measured the NER signal and performed *Z*-scans as a function of the pulse width for all samples. We did not consider the influence of the chirp sign in our model. NERs provide *B* values and *Z*-scans the normalized transmittance, ΔT_{pv} (or $n_{2,eff}$). In particular, CS_2 was chosen for calibration due to its well-known nonlinear parameters which permits a full calculation of the expected nonlinearity as function of the pulse width [6].

4.1. Pulse width determination

For fixed pulse energy, the laser irradiance can be changed by changing the pulse width. A chirped pulse amplified Ti:sapphire femtosecond laser system is very convenient for the present measurements because it can deliver pulses with different durations. Its pulse compressor gives the freedom of controlling the pulse width in a good time interval. This is achieved with a pair of gratings (1200 g/mm) mounted in a linear translation stage that allows moving one of the gratings by about 15 mm from the optimum pulse compression position. In order to measure the shortest pulse width, we carried out FROG measurements [22] with a commercial system (GRENOUILLE ECO Model 8-50) that is specified to go up to 500 fs (FWHM).

The pulse duration was determined by using the NER measurement in silica that has a pure electronic nonlinearity and its NER signal is inversely proportional to the pulse width provided that the pulse energy is kept constant. Therefore, one can obtain the pulse duration by NER signal of the silica and, simultaneously, follow the evolution of the solvent nonlinearity by its own NER signal. With this approach, it is only necessary to know the shortest pulse width which was about 60 fs (FWHM), measured by the GRENOUILLE. Pulses down to about 35 fs (laser bandwidth) can be obtained by a careful laser and compressor alignment, but we didn't bother to do that because the main purpose of the work was to explore longer pulses. Although the NER signal in silica gives a robust time width calibration, we confirmed the results with FROG measurements up to the limit of 500 fs. After a series of measurements, it was possible to plot an average pulse width as a function of pulse compressor setting as shown in Fig. 1. A parabolic curve was used to fit the data.

$$\tau(ps) = \left(\frac{d}{10.5}\right)^2 + 0.06, \tag{12}$$

where τ is the pulse width in ps and d, in millimeters, is the reading of the grating pair micrometer from the optimum compression position. It is important to mention that the micrometer reading does not give the actual distance change of the grating pair since the gratings are assembled in an angle at the top of the delay stage. With Eq. (1) it is possible to obtain the expected pulse width for each grating micrometer position which is necessary for *Z*-scan measurements since it is not a self-calibrated technique as NER is.

Optics EXPRESS

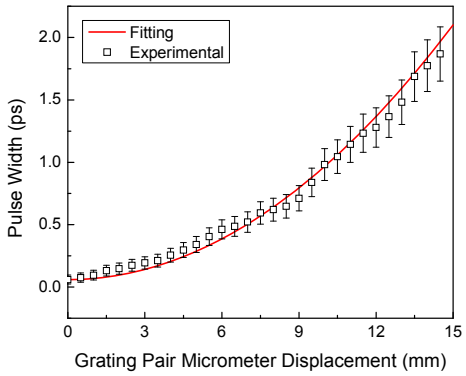

Fig. 1. Pulse width as function of the grating pair micrometer reading obtained with the silica NER signal. The line is the parabolic fitting curve given in Eq. (12).

For each measurement with constant pulse energy, we see the reference signal as two shoulders (two silica walls) and the solvent at the center, as Fig. 2 shows. Due to the presence of the slow reorientational nonlinearity, the effective solvent nonlinearity grows with the pulse width as can be noticed in the normalized NER curves. The normalized NER signals are obtained by considering that the silica nonlinearity is a constant independently of the pulse width.

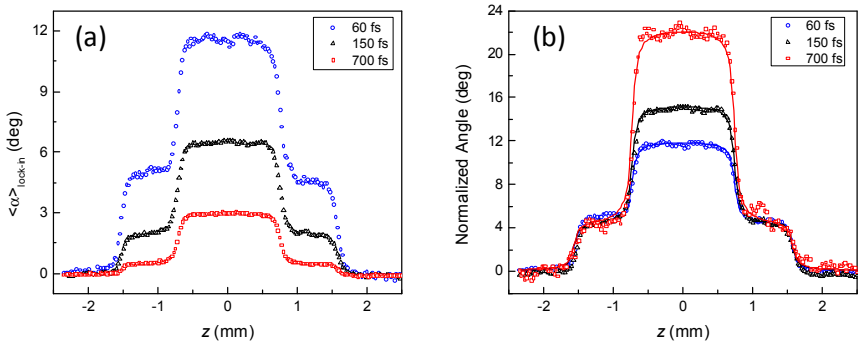

Fig. 2. (a) NER signals for acetone for three different pulse widths at the same pulse energy. (b) The NER signals normalized to a scale where the side shoulders (silica signal) are equals. The points are the experimental data and the lines are numerically calculated using the Eq. (11).

The fitting curves in Fig. 2 were obtained using Eq. (11) for each medium, considering the respective offset in terms of the z-position, its thickness, laser irradiance, n_o and the respective nonlinearity magnitude for silica (reference) and solvent (to be determined).

4.2. Measurements in CS_2

Z-scan measurements, shown as solid points in Fig. 3, were carried out with both linear and circular polarizations in order to experimentally provide $A_{eff} + B_{eff}/2$ and A_{eff} and their respective ratio. We worked at relatively small laser irradiance, such that ΔT_{pv} was kept smaller than ~0.1 for any pulse width, as a way to avoid the presence of the nonlinear absorption (I_0<10 GW/cm^2). The $n_{2,eff}$ curves for linear (solid line) and circular (dashed line) polarizations were numerically determined using Eq. (4) and the well-known optical parameters of CS_2 given in Table 1 [6]. In this table, $\tau_{r,m}$ and $\tau_{f,m}$ are the rise and fall times, respectively, for the m mechanism. The $n_{2,eff}$ curve for circular polarization can be calculated

Optics EXPRESS

by considering the symmetry properties *iso* (isotropic) and *re* (reorientational) of the response function, i. e. $\Delta n_{circ} = \Delta n^{iso}/1.5 = \Delta n^{re}/4$ [6].

Table 1. Values of the third-order response of CS_2 from [6]. The *B* values were determined from Eqs. (7) and (8)

Mechanism	$n_{2,m}$ (10^{-19}m^2/W)	$\tau_{r,m}$ (fs)	$\tau_{f,m}$ (fs)	B (10^{-21}m^2/V^2)	Symmetry
Electronic	1.5	*Inst.*	*Inst.*	2.79	*iso*
Collision	1.0	150	140	1.86	*iso*
Libration	7.6		450	31.4	*re*
Diffusive	18	150	1610	75.3	*re*

Using $n_{2,eff}$ for linear and circular polarizations, we can obtain the theoretical curves $A_{eff} + B_{eff}/2$ and A_{eff}, respectively. From them, it is possible to indirectly calculate the curve for B_{eff}, as also depicted in Fig. 4(a). The experimental errors were estimated from fluctuations in several independent measurements.

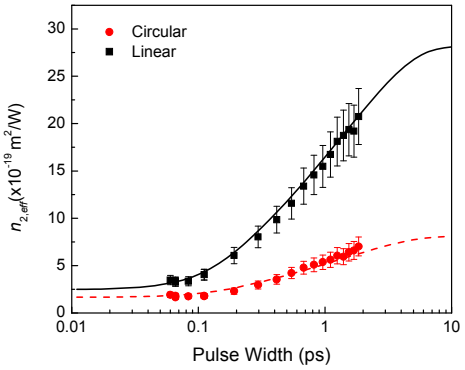

Fig. 3. Effective refractive nonlinearity for linear and circular polarization determined by the *Z*-scan technique in CS_2. The lines are the numerically calculated by Eq. (4) using the data of Table 1.

For short pulses $n_{2,eff}$(linear)/$n_{2,eff}$(circular)≈1.5 and for long pulses $n_{2,eff}$(linear)/$n_{2,eff}$(circular) = ΔT_{pv}(linear)/ΔT_{pv}(circular)≈3.5. The ratio for long pulse is not 4 due to the significant contribution of the isotropic nonlinearity. It is interesting to point out that the curves $A_{eff} + B_{eff}/2$ and B_{eff}, shown in Fig. 4(a) cross at a particular pulse width (about 100 fs). At this point, the ratio of ΔT_{pv} for linear and circular polarization is exactly 2, as seen in Fig. 4(b).

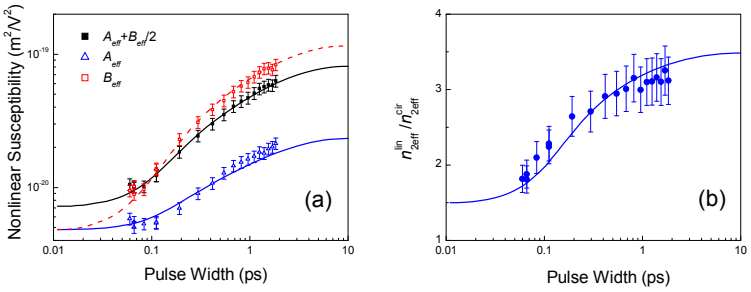

Fig. 4. (a) Nonlinear susceptibilities determined from nonlinear refraction of CS_2. The experimental *Z*-scan points of $A_{eff} + B_{eff}/2$ and A_{eff} were obtained with linear and circular polarizations, respectively. The experimental B_{eff} points were determined indirectly from $A_{eff} + B_{eff}/2$ and A_{eff} points. The theoretical lines were calculated with Eq. (4). (b) Ratio between ΔT_{pv}(linear)/ΔT_{pv}(circular) obtained with *Z*-scan measurements. The theoretical ratio (line) was obtained with Eq. (4).

Optics EXPRESS

A similar study using NER measurements instead of *Z*-scan was also performed in CS_2. In this case, we experimentally measured effective *B* values and, using our empirical model, Eq. (9), we obtained the respective B_{fast}, B_{slow} and τ_0, where B_{fast} turns out to be the sum of *isotropic* contributions (electronic + collision) and B_{slow} is the sum of *reorientational* (libration + diffusive) contributions (Table 1). A good adjust to the experimental data could be obtained using $B_{fast} = 4.5 \times 10^{-21} m^2/V^2$, $B_{slow} = 110 \times 10^{-21} m^2/V^2$ and $\tau_0 = 1.3$ ps. The response times obtained with our model probably correspond to weighted values which have mainly contributions from the diffusive and the libration mechanisms. Considering this hypothesis for CS_2, we expect an weighted response time of about 1.3 ps using the data of the Table 1 ((7.6*0.45 + 18*1.61)/(7.6 + 18)). Similarly, we can also trace the curve for A_{eff} and $A_{eff} + B_{eff}/2$ using the correct conversion between *B* and *A,* Eq. (7) and (8), for the respective symmetry *iso* and *re* processes. For NER measurements, we have used tightly focused beam, and in this way, higher laser irradiances (I_0<60 GW/cm^2) are produced in comparison to those used for Z-scan measurements (thin samples).

As seen in the Figs. 4 and 5, *Z*-scan and NER measurements show good agreement. Basically, even with the simplicity of our model and the presence of only one characteristic response time, there are good agreement between the experimental data and the theoretical curves, as seen in Fig. 5. There are some mismatching in certain pulse width regions, but not so severe to fade the potential of our model. It is interesting to stress that with our empirical model it is possible to predict other nonlinear susceptibilities curves just measuring one of nonlinear susceptibility (A_{eff} or B_{eff}) curve, which in our case was B_{eff}. Also, the experimental errors (~10-15%) in B_{eff}, not plotted in the Fig. 5, were estimated from fluctuations among several independent measurements.

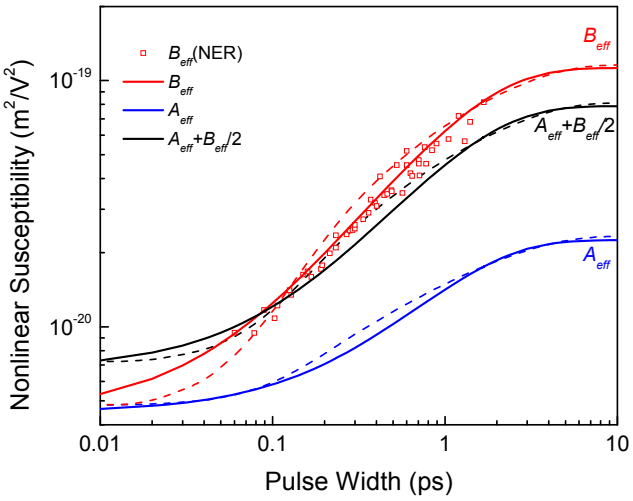

Fig. 5. Experimental points of B_{eff} for CS_2 obtained with NER measurements. The nonlinear susceptibility curves were determined with Eq. (4) (dashed lines) and with our empirical model (solid lines). We did not use error bars in the experimental points just to help to see the lines.

4.3. Measurement in other solvents

Since our empirical model works adequately for CS_2, we extended our study to other solvents using NER and Z-scan measurements. We performed NER measurements to obtain B_{eff} and indirectly obtained A_{eff} and $A_{eff} + B_{eff}/2$ curves as function of pulse width, as Figs. 6 and 8 show. We did not use error bars in Fig. 6 to facilitate the view of each solvent. In general, the error in the measurement was estimated to be about 10%-15%, due to statistical fluctuation in the experimental values measured. Here we worked with no noticeable two-photon absorption.

Optics EXPRESS

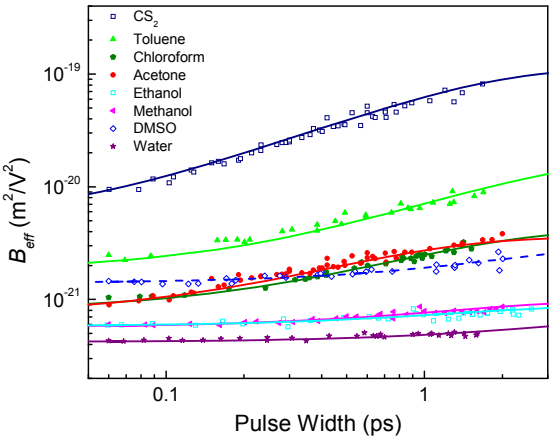

Fig. 6. Experimental B_{eff} values of the 8 solvents obtained with NER measurements (points). The lines are theoretical curves given by Eq. (9).

It is possible to calculate, with our model, the expected nonlinear refraction for all solvents using Eq. (5) and the correspondent $n_{2,fast}$ and $n_{2,slow}$ calculated from B by the correspondent conversion Eqs. (7) and (8) (Table 2) as shown in Fig. 7. Using B_{eff} curves obtained with our model, it is possible to plot the curves for A_{eff} using Eq. (10) and also $A_{eff} + B_{eff}/2$, as shown in Fig. 8. These two curves are important to determine the ratio between $(A_{eff} + B_{eff}/2)/A_{eff}$, as we will see later.

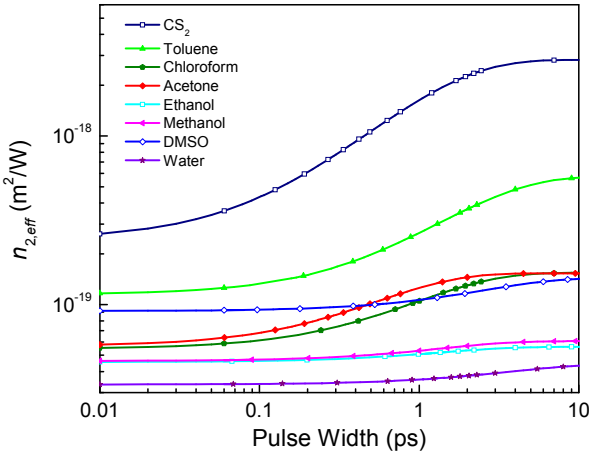

Fig. 7. Effective n_2 values obtained with our model, Eq. (5) using the data of Table 2, for the solvents of Fig. 6. The points in the graph are just to help to distinguish the solvents, they are not experimental measurements.

An interesting characteristic seen in the curves of Fig. 8 is that the curve $A_{eff} + B_{eff}/2$ sometimes crosses (sometimes not) the curve B_{eff} at a given pulse width. It happens for CS_2 (~100 fs), toluene (~400 fs), chloroform (~1 ps) and acetone (~350 fs). At these pulse widths, the ratio between ΔT_{pv} obtained with Z-scan for linear and circular polarization is exactly 2. In other words, the ΔT_{pv} for circular polarization is half of that for linear polarization. For the other 4 solvents, we could not see these crossing points and consequently $A_{eff} + B_{eff}/2$ curves will be always above the B_{eff} curves.

Optics EXPRESS

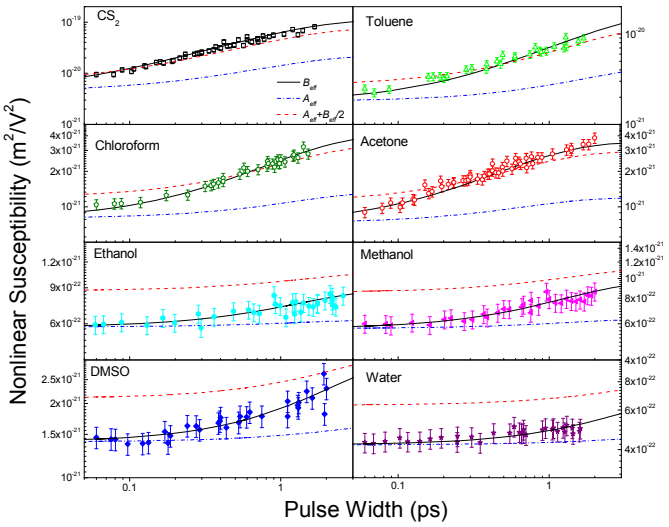

Fig. 8. Experimental B_{eff} values of all 8 solvents obtained with NER measurements (points). By fitting the experimental B_{eff} data with Eq. (9) (black solid lines) other nonlinear susceptibilities can be obtained, A_{eff} (blue dash lines) and $A_{eff} + B_{eff}/2$ (red dashed lines).

To summarize, Table 2 shows all nonlinear parameters obtained by our model. Except for CS_2, which *fast* (*istropic*) and *slow* (*reorientational*) nonlinearities match pretty well those found in the literature [6], other solvents have few experimental data available, particularly for long pulses, which make the comparison difficult. But, if we consider that the nonlinearity depends on the pulse duration and that there is a relatively broad dispersion of the values found in the literature, our data are in good agreement to those expected. It is important to point out that with our model the expected nonlinearity for a long pulse corresponds to the sum of the *fast* and *slow* values. For example, the expected value for long pulses in CS_2 is 281-310 × 10^{-20}m^2/W [6,11]. Pulses with more than 10 ps can be considered long for CS_2. For comparison, we list in Table 2 some of the data found in the literature obtained with 16 ps [11] and 35 ps [23] laser pulse at 1064 nm and 532 nm, respectively, and for 110 fs at 800 nm [24].

Table 2. Fitting parameters of third-order response of all solvents. Some data from literature, Ref [24]. [a] [11], [b] [23], [c] and [6][d]. Here, B is in 10^{-21}m^2/V^2 and n_2 is in 10^{-20}m^2/W and τ is in ps

Solvent	n_0	B_{fast}	$n_{2,fast}$	B_{slow}	$n_{2,slow}$	$n_{2,\text{total}}$	$n_{2,\text{total}}$	τ_0
CS_2	1.63	4.5	23.9 {25[d]}	110	260 {256d}	284	310[b], 281[d]	1.3
Toluene	1.49	1.8	11.5 {14.0[a]}	16	45.2	57	93[b], 108[c]	2.5
DMSO	1.47	1.4	9.15	1.8	5.23	14	28[b]	3.0
Chloroform	1.44	0.8	5.45 {9.37[a]}	3.0	9.1	15	38[b], 33[c]	1.4
Acetone	1.35	0.73	5.66 {9.34[a]}	2.8	9.6	15	23[b], 22[c]	0.8
Methanol	1.32	0.57	4.62	0.4	1.44	6.1	18[b]	1.5
Ethanol	1.36	0.58	4.43 {10.9[a]}	0.3	1.02	5.5	18[b]	1.5
Water	1.33	0.42	3.35	0.3	1.06	4.4	14[b]	4.0

We did not specify the error values in the data of Table 2 just to save space in the columns. To be conservative, errors in the values are estimated to be about 20% based on

Optics EXPRESS

uncertainties in the irradiance and pulse width determinations, added to statistical fluctuation in the experimental values measured.

Comparing to results found in the literature, in [24], for example, Krishna *et al*. performed *Z*-scan measurement with 110 fs pulse duration at 800 nm. As our model predicts, the solvent carries contributions of isotropic and others slow reorientational nonlinearities at this pulse width, and so, it is not totally correct to attribute the n_2 values measured in [24] as pure electronic nonlinearity. The value of n_2 at 110 fs should be slightly greater than that obtained with our model. For longer pulses, our data are in general slightly smaller than those found in the literature [11,22]. Considering the typical uncertainty on the nonlinear refraction determination among different techniques, laser types, wavelength, etc., these discrepancies are acceptable. In fact, Krishna *et al*. [24] also presented measurements with long pulses (30 ps at 532 nm), and the values found also show significant discrepancies (higher values) with our data and with others from literature [11,23]. In [24], the measurements were carried out in the presence of nonlinear absorption, at 532 nm, where dispersion helps to explain the upper values.

The final test of our model is the ratio of $n_{2,eff}$ for linear and circular polarizations, that can be easily obtained with *Z*-scan measurements. In order to test the self-consistency of our model, we calculate the ratio $(A_{eff} + B_{eff}/2)/A_{eff}$ which is exactly, $n_{2,eff}^{lin}/n_{2,eff}^{circ}$. Figure 9 shows that the experimental ratios obtained with the *Z*-scan technique are very similar to those determined with our model, indicating that both the curves of A_{eff} and $A_{eff} + B_{eff}/2$ are correct. We also can organize these 8 solvents in two groups, one where the ratio is larger than 2 and another that is not. In the first group, we have CS_2, toluene, chloroform and acetone, and in the second group, ethanol, methanol, DMSO and water. Basically, when these two curves do not cross each other, it means that the contribution of the reorientational nonlinearity is lower in comparison to the fast isotropic nonlinearity.

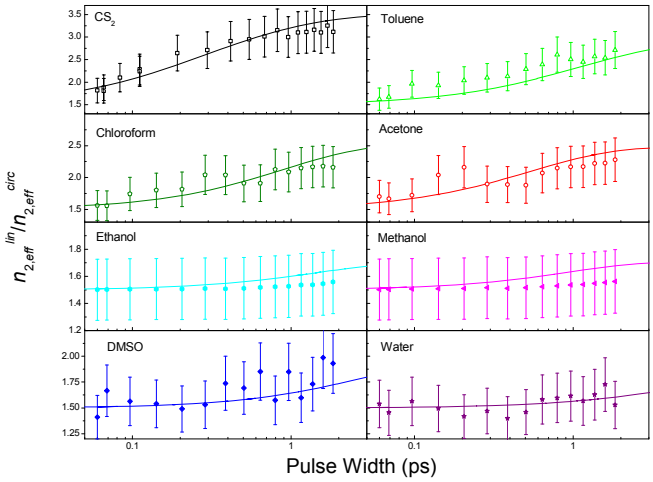

Fig. 9. The ratio $n_{2,eff}^{lin}/n_{2,eff}^{circ}$ for all solvents obtained with the *Z*-scan technique. The lines are the theoretical fittings based on our model, $n_{2,eff}^{lin}/n_{2,eff}^{circ} = (A_{eff} + B_{eff}/2)/A_{eff}$.

For *Z*-scan and NER measurements we worked at lower laser irradiance as possible, typical value of I_0<50 GW/cm^2 and I_0<250 GW/cm^2, respectively, for any pulse width. No significant nonlinear absorptions were observed with these irradiances.

5. Conclusions

In summary, we have measured the NER signal of 8 different solvents as a function of pulse duration. We found that all solvents present reorientational (slow) nonlinearities in addition to the isotropic (fast) one. We proposed an empirical model which was able to explain the pulse

Optics EXPRESS

width dependence and also to discriminate isotropic and reorientational nonlinearities. In addition, it was possible to found characteristic response times of the solvents. CS_2 was the solvent used as reference to test the proposed model. Using the tensor nature of the third-order nonlinearity in isotropic samples, it was possible to predict several interesting consequences of the nonlinearity. These results are important from the material's characterization point of view since the literature lacks nonlinearity data related to the pulse width dependence.

Funding

This research was supported by Fundação de Amparo à Pesquisa do Estado de São Paulo (FAPESP, Grant: 2013/23999-3) and Conselho Nacional de Desenvolvimento Científico e Tecnológico (CNPq, Grant: 475428/2013-7).